SLIDING MODE CONTROL APPLIED TO WAYPOINT-BASED GUIDANCE OF A MULTIROTOR AERIAL VEHICLE

José Agnelo Bezerra* , Igor Afonso Acampora Prado* , Davi Antônio dos Santos*

*Praça Marechal Eduardo Gomes, 50
Vila das Acácias
São José dos Campos, São Paulo, Brasil

Email: agnelo@ita.br, igorap@ita.br, davists@ita.br

Abstract— The present paper deals with the waypoint-based guidance of a multirotor aerial vehicle in the presence of a bounded wind disturbance. A discrete-time quasi-sliding mode control (SMC) strategy is adopted, which assures finite-time stability to the guidance. In the proposed control loop, the position command is transmitted to the controller as a sequence of tridimensional waypoints. The current waypoint of the sequence is detected as soon as the vehicle enters inside a virtual sphere centered at it. At this moment, the next waypoint commanded is made active. This switching-waypoint rule is repeated until the final waypoint is activated, at which the vehicle is commanded to hover. The finite-time stability is assured by the reaching law of SMC, which keeps the multirotor's position close to the next waypoint of the reference trajectory. The resulting control law is simple to implement in an embedded real-time system. The proposed method is evaluated on computational simulations and trajectories very close to the reference were achieved, proving its efficiency and robustness against a bounded random wind disturbance.

Keywords— Robust control, sliding mode control, multirotor aerial vehicles, waypoint-based guidance.

Resumo— Este artigo lida com o problema de guiamento por *waypoints* de veículos aéreos multirotores na presença de um distúrbio de vento. A fim de solucionar o problema, propõe-se a formulação de um controlador por modos deslizantes em tempo discreto. A entrada de comando para o controlador consiste em uma sequência de *waypoints* tridimensionais. Um *waypoint* é detectado assim que o veículo entra em uma esfera virtual com centro neste ponto e raio especificado. No mesmo instante, o algoritmo já passa a buscar o próximo *waypoint* da trajetória. Essa regra é repetida até que o veículo alcance o último *waypoint*, onde ele é comandado a manter-se em voo pairado. A regra de aproximação utilizada garante ao sistema estabilidade em tempo finito, o que implica que a posição do robô é levada e mantida numa região em torno do próximo *waypoint* da trajetória de referência. A lei de controle resultante é simples de ser embarcada em um sistema físico em tempo real. O método proposto é avaliado em simulações computacionais e foram obtidas trajetórias muito próximas à referência, o que comprova sua eficiência e robustez contra uma perturbação aleatória e limitada de vento.

Palavras-chave— Controle robusto, controle por modos deslizantes, veículos aéreos multirotores, guiamento por *waypoints*.

1 Introduction

Waypoint-based guidance for multirotor aerial vehicles (MAV) is already a popular technology, being available even in open-source/open-hardware autopilots systems, such as the Mission Planner/Ardupilot Mega. Basically, it consists in controlling the position of a vehicle so as to make it approximately pass through desired positions, which we call waypoints.

Many papers have investigated the waypoint-based guidance, however considering other types of autonomous vehicles: (Petersen et al., 2013; Lenain et al., 2006; Almeida, 2008; Bousson and Machado, 2013; Richards and How, 2002). The paper (Nagaty et al., 2013) used a nonlinear control technique to solve the multirotor trajectory tracking problem. In this work, the outer loop controller generates the reference trajectories for the inner loop controller in order to reach the desired waypoint. More recently, (Santos et al., 2015) treated the problem of waypoint-based guidance an MAV using a model predictive controller (MPC) and introduced a strategy for avoidance of a static obstacle. This technique is able to respect constraints on the vehicle's position and thrust vector during the guidance mission. The present paper proposes a method based on the sliding model control (SMC) strategy for waypoint-based guidance of an MAV subject to a bounded wind disturbance. Different of the MPC method investigated in (Santos et al., 2015), the proposed control law assures robustness against bounded disturbances.

The remaining text is organized in the following manner. Section 2 enunciates the waypoint-based multirotor guidance problem. Section 3 presents a sliding mode controller for solving the guidance problem defined in Section 2. Section 4 shows the simulation results. Finally, Section 5 presents the concluding remarks.

2 Problem Definition

Consider a quadrotor and two Cartesian Coordinate Systems (CCS) (see Figure 1). The body CCS $S_{\mathrm{B}} = \{X_{\mathrm{B}}, Y_{\mathrm{B}}, Z_{\mathrm{B}}\}$ is fixed on the vehicle's frame at its center of mass (CM). The ground CCS $S_{\mathrm{G}} = \{X_{\mathrm{G}}, Y_{\mathrm{G}}, Z_{\mathrm{G}}\}$ is fixed at a known point O on Earth. For simplicity, the time dependence of all vectors will be omitted from now on.

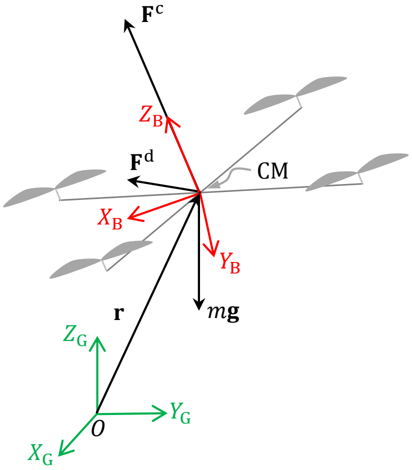

Figure 1: Cartesian coordinate systems and forces acting on a multirotor aerial vehicle.

Assume that S_G is an inertial frame. In this case, an immediate application of the second Newton's law gives the following dynamics model for the translational motion of the vehicle represented in S_G:

$$\ddot{\mathbf{r}}_G = \frac{1}{m}\left(\mathbf{F}_G^c + \mathbf{F}_G^d\right) + \mathbf{g}_G, \tag{1}$$

$$\mathbf{F}_G^c = \mathbf{D}^T \mathbf{F}_B^c, \tag{2}$$

where $\mathbf{r}_G \in \mathbb{R}^3$ denotes the position $\mathbf{r}$ of CM represented in S_G; $\mathbf{F}_G^c, \mathbf{F}_B^c \in \mathbb{R}^3$ are the total thrust force vector $\mathbf{F}^c$ represented in S_G and S_B, respectively; $\mathbf{F}_G^d \in \mathbb{R}^3$ is the disturbance force vector $\mathbf{F}^d$ represented in S_G; $\mathbf{g}_G \triangleq \begin{bmatrix} 0 & 0 & -g \end{bmatrix}^T$ is the gravitational acceleration vector represented in S_G, with g denoting its magnitude; m is the mass of the vehicle; and $\mathbf{D} \in SO(3)$ is the attitude matrix representing the attitude of S_B w.r.t. S_G.

Assume that the unknown disturbance force is limited, *i.e.*,

$$\mathbf{F}_{min}^d \leq \mathbf{F}_G^d \leq \mathbf{F}_{max}^d, \tag{3}$$

where $\mathbf{F}_{min}^d, \mathbf{F}_{max}^d \in \mathbb{R}^3$ are, respectively, the minimum and maximum disturbance forces represented in S_G. These bounds are assumed to be known.

Define the jth waypoint $\mathbf{w}_j \in \mathbb{R}^3$ as a position vector represented in S_G. Assume that a sequence $\{\mathbf{w}_1, \mathbf{w}_2, ..., \mathbf{w}_q\}$ of q waypoints is known before-hand. Therefore, define the reference trajectory $\bar{\mathbf{r}}$ for the vehicle's flight as the sequence of line segments linking the waypoints, as illustrated in Figure 2.

Problem 1. Consider an MAV with translation dynamics described by (1)-(2), subject to a disturbance force $\mathbf{F}_G^d$ modeled by (3). The waypoint-based guidance problem consists in finding a feedback control law for $\mathbf{F}_G^c$ that makes the vehicle's position $\mathbf{r}_G$ follow the reference trajectory $\bar{\mathbf{r}}$.

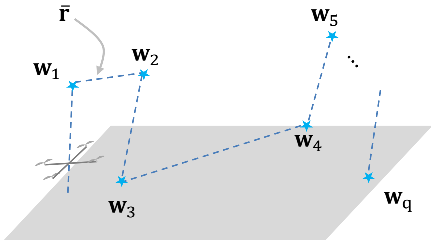

Figure 2: A waypoint-based reference trajectory for a multirotor aerial vehicle.

3 Problem Solution

This section presents a solution to Problem 1 based on a discrete-time SMC strategy proposed by (Bartoszewicz, 1998).

3.1 State-Space Model

In order to obtain the design model, consider the following assumption.

Assumption 1. Let $\bar{\mathbf{F}} \in \mathbb{R}^3$ denote the thrust command computed by the guidance law defined in Problem 1. Assume that there is no deviation between this command and the real thrust force, i.e., $\mathbf{F}_G^c \equiv \bar{\mathbf{F}}$.

The following design model can be defined from equation (1) and Assumption 1:

$$\ddot{\mathbf{r}}_G = \frac{1}{m}\bar{\mathbf{F}} + \frac{1}{m}\mathbf{F}_G^d + \mathbf{g}_G. \tag{4}$$

Define the state vector $\mathbf{x} \triangleq \left[\mathbf{r}_G^T \; \dot{\mathbf{r}}_G^T\right]^T$, the controlled output vector $\mathbf{y} \triangleq \mathbf{r}_G$, and the control input vector:

$$\mathbf{u} \triangleq \frac{1}{m}\bar{\mathbf{F}} + \mathbf{g}_G. \tag{5}$$

The following discrete-time translational dynamics model can be obtained by discretizing (4)-(5) with the ZOH method:

$$\mathbf{x}_{k+1} = \mathbf{A}\mathbf{x}_k + \mathbf{B}\mathbf{u}_k + \mathbf{f}_k, \tag{6}$$

$$\mathbf{y}_k = \mathbf{C}\mathbf{x}_k, \tag{7}$$

where $T \in \mathbb{R}_+$ is the sampling time and

$$\mathbf{A} = \begin{bmatrix} \mathbf{I}_3 & T\mathbf{I}_3 \\ \mathbf{0}_{3\times3} & \mathbf{I}_3 \end{bmatrix} \in \mathbb{R}^{6\times6}, \tag{8}$$

$$\mathbf{B} = \begin{bmatrix} \frac{T^2}{2}\mathbf{I}_3 \\ T\mathbf{I}_3 \end{bmatrix} \in \mathbb{R}^{6\times3}, \tag{9}$$

$$\mathbf{C} = \begin{bmatrix} \mathbf{I}_3 & \mathbf{0}_{3\times3} \end{bmatrix} \in \mathbb{R}^{3\times6}. \tag{10}$$

The vector $\mathbf{f}_k$ is the discrete-time disturbance. It is given by

$$\mathbf{f}_k = \frac{1}{m}\mathbf{B}\mathbf{F}_G^d. \tag{11}$$

ISSN 2525-8311

3.2 Sliding Surface

Consider the vector $\mathbf{s}_k \in \mathbb{R}^3$ as the composition of three sliding surfaces for the model (6), each one related to a component of the control input $\mathbf{u}_k$.

$$\mathbf{s}_k = \boldsymbol{\sigma}^{\mathrm{T}} \left(\mathbf{x}_k - \bar{\mathbf{x}}_k \right), \tag{12}$$

with $\boldsymbol{\sigma} = \begin{bmatrix} \mathbf{I}_3 & \mathbf{I}_3 \end{bmatrix}^{\mathrm{T}} \in \mathbb{R}^{6\times 3}$ and $\bar{\mathbf{x}}_k = \begin{bmatrix} \mathbf{w}_j^{\mathrm{T}} & \mathbf{0}_{1\times 3} \end{bmatrix}^{\mathrm{T}} \in \mathbb{R}^6$.

Define a disturbance vector $\mathbf{d}_k \in \mathbb{R}^3$ to be

$$\mathbf{d}_k = \boldsymbol{\sigma}^{\mathrm{T}} \mathbf{f}_k. \tag{13}$$

Once $\boldsymbol{\sigma}^{\mathrm{T}}\mathbf{B}$ is positive definite, it is possible to rewrite the boundaries of the disturbance force $\mathbf{F}_{\mathrm{G}}^{\mathrm{d}}$ in terms of $\mathbf{d}_k$. Therefore, we left-multiply both sides of equation (3) by the term $\frac{1}{m}\boldsymbol{\sigma}^{\mathrm{T}}\mathbf{B}$, yielding

$$\mathbf{d}_{\min} \leq \mathbf{d}_k \leq \mathbf{d}_{\max}, \tag{14}$$

where

$$\mathbf{d}_{\min} \triangleq \frac{1}{m}\boldsymbol{\sigma}^{\mathrm{T}}\mathbf{B}\mathbf{F}_{\min}^{\mathrm{d}}, \tag{15}$$

$$\mathbf{d}_{\max} \triangleq \frac{1}{m}\boldsymbol{\sigma}^{\mathrm{T}}\mathbf{B}\mathbf{F}_{\max}^{\mathrm{d}}. \tag{16}$$

From the bounds $\mathbf{d}_{\min}$ and $\mathbf{d}_{\max}$, one can define a mean $\mathbf{d}_0 \in \mathbb{R}^3$ and a deviation $\boldsymbol{\delta}_{\mathrm{d}} \in \mathbb{R}^3$ as:

$$\mathbf{d}_0 \triangleq \frac{\mathbf{d}_{\max} + \mathbf{d}_{\min}}{2}, \tag{17}$$

$$\boldsymbol{\delta}_{\mathrm{d}} \triangleq \frac{\mathbf{d}_{\max} - \mathbf{d}_{\min}}{2}. \tag{18}$$

3.3 Waypoint Commutation

Consider that, at a certain instant k, the current waypoint of the vehicle's flight is $\mathbf{w}_j$. Also, we define the discrete time $k_j \in \mathbb{Z}_+$ at which the waypoint $\mathbf{w}_j$ is detected by the system. Initially, we set $j = 1$ and $k_0 = 0$.

Before presenting the waypoint detection rule, define a waypoint detection sphere $\mathcal{B}_{\mathbf{w}_j}(\lambda) \subset \mathbb{R}^3$ as an Euclidean ball centered at $\mathbf{w}_j$, with radius $\lambda \in \mathbb{R}_+$, and consider that from now on, λ will be called the waypoint detection radius. Therefore, as soon as the following condition is verified:

$$\mathbf{y}_k \in \mathcal{B}_{\mathbf{w}_j}(\lambda), \tag{19}$$

the waypoint $\mathbf{w}_j$ is detected and the system starts to pursuit the next waypoint $\mathbf{w}_{j+1}$. This rule is repeated up to the last waypoint $\mathbf{w}_q$. At this moment, the parameter k_j is set as the current time k and the reference state vector is updated to $\bar{\mathbf{x}}_k = \begin{bmatrix} \mathbf{w}_j^{\mathrm{T}} & \mathbf{0}_{1\times 3} \end{bmatrix}^{\mathrm{T}}$.

3.4 Control Law

Consider the following reaching law (Bartoszewicz, 1998):

$$\mathbf{s}_{k+1} = \bar{\mathbf{s}}_{k+1} + \mathbf{d}_k - \mathbf{d}_0, \tag{20}$$

where $\bar{\mathbf{s}}_{k+1} \in \mathbb{R}^3$ is the desired trajectory for $\mathbf{s}_{k+1}$.

The vector $\bar{\mathbf{s}}_{k+1}$ is a predefined function in discrete time. It must satisfy some conditions to assure robustness [for details, see in (Bartoszewicz, 1998)]. In this paper, it is assumed that:

$$\bar{s}_k^i = \begin{cases} \frac{\tau^i + k_{j-1} - k}{\tau^i} s_0^i, & \text{if } k < \tau^i + k_{j-1} \\ 0, & \text{if } k \geq \tau^i + k_{j-1} \end{cases} \tag{21}$$

where s_0^i and $\bar{s}_k^i$ represent the i-th element of the vectors $\mathbf{s}_0$ and $\bar{\mathbf{s}}_k$, respectively, for $i \in \{1, 2, 3\}$. $\boldsymbol{\tau} \in \mathbb{R}^3$ is a vector of discrete times that must satisfy the condition:

$$\tau^i < \frac{s_0^i}{2\delta_{\mathrm{d}}^i}. \tag{22}$$

where δ_{d}^i is the ith component of $\boldsymbol{\delta}_{\mathrm{d}}$.

One can see, by equation (21), that the parameter $\boldsymbol{\tau}$ determines how fast $\mathbf{s}_k$ must converge to zero, which establishes the vehicle's speed. From now on, it will be called as the time of convergence.

In order to obtain the control law, equation (6) is left-multiplied by $\boldsymbol{\sigma}^{\mathrm{T}}$ and the result is an expression for $\mathbf{s}_{k+1}$. Replacing this equation into (20) and isolating the control input $\mathbf{u}_k$, we obtain

$$\mathbf{u}_k = (\boldsymbol{\sigma}^{\mathrm{T}}\mathbf{B})^{-1} \left[\bar{\mathbf{s}}_{k+1} - \boldsymbol{\sigma}^{\mathrm{T}}\mathbf{A}\mathbf{x}_k + \boldsymbol{\sigma}^{\mathrm{T}}\bar{\mathbf{x}}_{k+1} - \mathbf{d}_0 \right]. \tag{23}$$

3.5 Computation of the Commands to the Plant

As soon as the control input vector $\mathbf{u}_k$ is calculated, it can be converted into the corresponding thrust command $\bar{\mathbf{F}}$ by using equation (5). However, this force command is not sufficient as an output of a guidance law for a multirotor aerial vehicle. In fact, the system has to provide two commands for the quadrotor's internal control loop: a reference for the magnitude of the total thrust vector and an attitude reference. The complete explanation of how these commands are calculated by the controller can be found in (Prado and Santos, 2014).

4 Simulation Results

This section aims at evaluating the proposed guidance method using computational simulations. Subsection 4.1 describes the simulation environment, while Subsection 4.2 presents the results.

ISSN 2525-8311

4.1 System Simulation

The proposed guidance system is simulated in MATLAB/Simulink with a six-degree-of-freedom dynamics model of attitude and position, considering a quadrotor in "plus" configuration with the parameters listed in Table 1.

In the (internal) attitude control loop, a saturated proportional-derivative control law with proportional gain $K_p = 40$ and derivative gain $K_d = 2$ is used. On the other hand, in the (external) position control loop, the SMC proposed in Section 3 is adopted. Table 2 presents the SMC parameters used in the simulations.

The disturbance force $\mathbf{F}_\mathrm{G}^\mathrm{d}$ is chosen to simulate a moderate wind. It is modeled by a zero-mean Gaussian noise trucated by the bounds established in (3), with covariance $\mathbf{Q} = \mathrm{diag}(0.01, 0.01, 0.005625)$.

4.2 Simulation results

The proposed guidance strategy is evaluated in the simulation of a complete mission, with takeoff, tracking of some given waypoints and landing. So, at the start time, the quadrotor rests at point O and the mission consists of tracking the following five waypoints: $\mathbf{w}_1 = [\ 0\ \ 0\ \ 3\ ]^\mathrm{T}$m, $\mathbf{w}_2 = [\ 3\ \ 0\ \ 3\ ]^\mathrm{T}$m, $\mathbf{w}_3 = [\ 3\ \ 3\ \ 3\ ]^\mathrm{T}$m, $\mathbf{w}_4 = [\ 6\ \ 3\ \ 3\ ]^\mathrm{T}$m, and $\mathbf{w}_5 = [\ 6\ \ 3\ \ 0\ ]^\mathrm{T}$m.

The time of convergence $\boldsymbol{\tau}$ is chosen in order to respect the condition (22) for all the trajectory segments.

Figure 3 shows the trajectory executed by the vehicle as a continuous blue line. The waypoints are represented by stars, with the last one in red. The reference trajectory is represented by the dashed red lines.

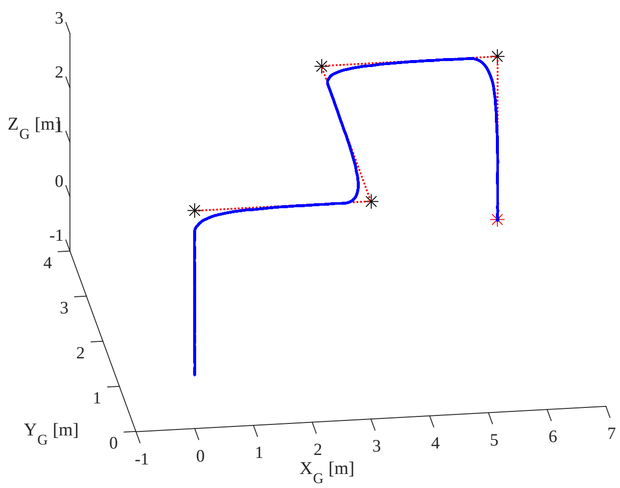

Figure 3: 3D path performed by the quadrotor in simulation.

Figures 4, 5, and 6 presents the evolution of each component of the vector $\mathbf{s}_k$ during the simulation (continuous red lines). The straight lines represent the subset of states such that $s_k^i = 0$ relative to some waypoint, for $i \in \{1, 2, 3\}$.

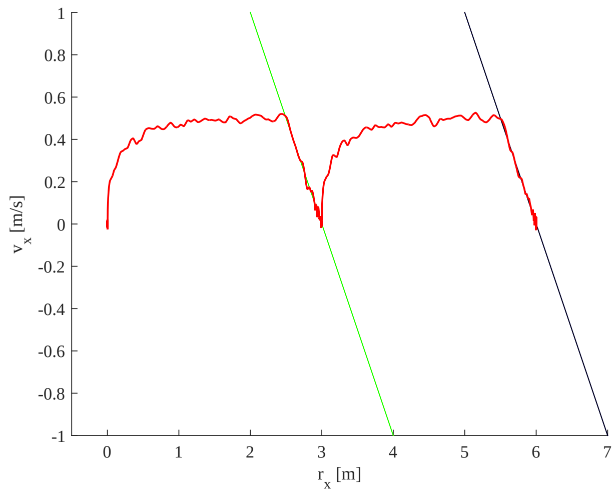

Figure 4: Phase diagram in the X_G direction. The green line represents the sliding surface relative to $\mathbf{w}_2$ and the black one refers to $\mathbf{w}_4$.

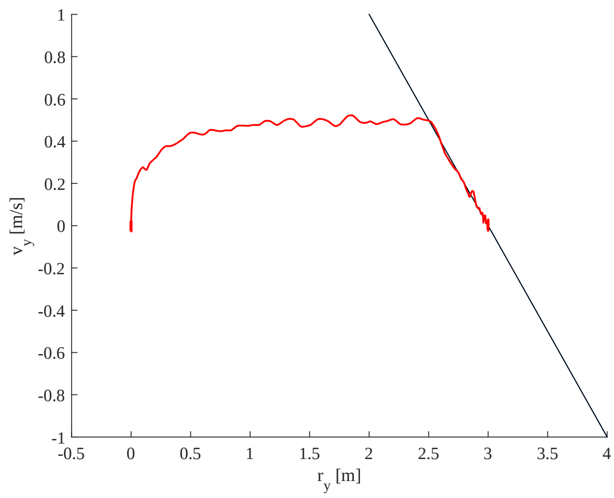

Figure 5: Phase plane in the Y_G direction. The black line represents the sliding surface relative to $\mathbf{w}_3$.

One can note that the controller effectively conducts the states to the sliding lines $s_k^i = 0$, which corresponds to tracking the vehicle toward the next waypoint. Figure 7 presents a detail of Figure 6 with the behavior of states near a sliding surface. One can be seen that the SMC maintains the states inside a bounded region close to a given waypoint, since: $-\delta_\mathrm{d}^i \leq s_k^i \leq \delta_\mathrm{d}^i$, $i \in \{1, 2, 3\}$.

Figure 8 shows the control input values calculated by the SMC during the simulation. The continuous black lines represent the desired bounds to the control input in X_G and Y_G directions. The resulting controls respect the tight limits on X_G and Y_G directions, which are set for safety and maneuverability reasons. On the Z_G direction, the vehicle commonly has a higher propulsion capability, so the respective controls are inside the

Table 1: Parameters of the quadrotor considered on simulations.

Mass: $m = 1$ kg
Inertia matrix: $\mathbf{J} = \text{diag}\{0.0171, 0.0171, 0.0286\}$ kgm^2
Frame radius: $l = 0.2$ m
Motor-drive time constant: $\tau = 0.01$ s
Motor's maximum speed: $\omega_{\text{max}} = 10000$ rpm
Rotor's force constant: $k_f = 3.13 \times 10^{-5}$Ns^2
Rotor's moment constant: $k_t = 7.5 \times 10^{-7}$Nms^2

Table 2: Parameters of the SMC controller used in the position control.

Sampling time: $T = 0.1$ s
Waypoint detection radius: $\lambda = 0.5$ m
Minimum disturbance force: $\mathbf{F}^{\text{d}}_{\text{min}} = [-0.2, -0.2, -0.15]^{\text{T}}$ N
Maximum disturbance force: $\mathbf{F}^{\text{d}}_{\text{max}} = [0.2, 0.2, 0.15]^{\text{T}}$ N
Time of convergence $\boldsymbol{\tau} = [60, 60, 60]^{\text{T}}$s

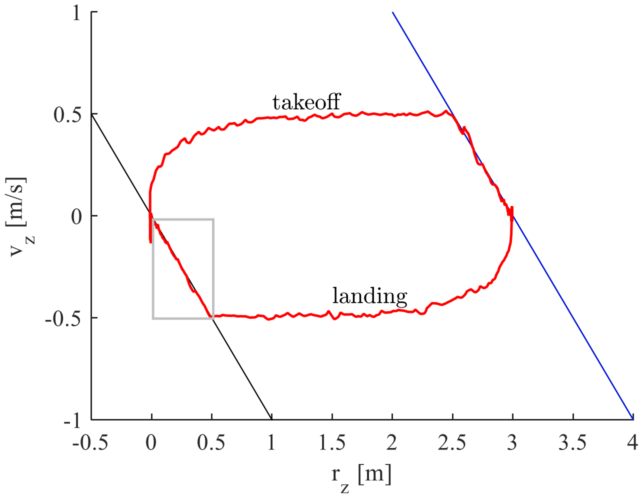

Figure 6: Phase diagram in the Z_{G} direction. The blue line represents the sliding surface relative to $\mathbf{w}_1$ (takeoff) and the black one refers to $\mathbf{w}_5$ (landing).

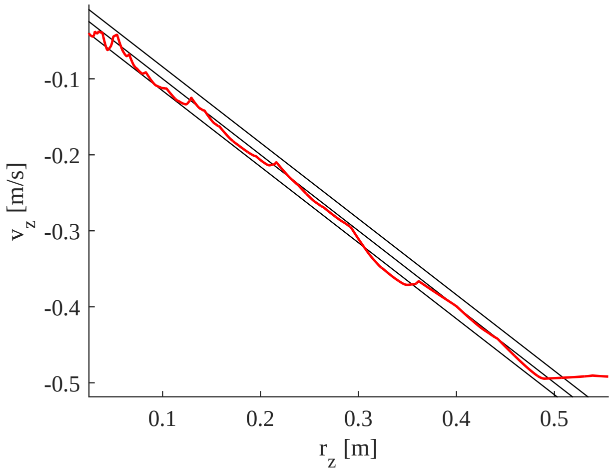

Figure 7: Detail of Figure 6 which refers to the landing (waypoint $\mathbf{w}_5$). The external continuous black lines represent the surfaces with $s^3_k = \delta^3_{\text{d}}$ and $s^3_k = -\delta^3_{\text{d}}$.

bounds. For more information about thrust vector constraints, see the references (Santos et al., 2013) and (Prado and Santos, 2014).

5 Conclusions and Future Works

The present paper proposed a sliding mode controller (SMC) for waypoint-based guidance of a multirotor aerial vehicle subject to a bounded wind disturbance force.

The results presented in section 4 show that the strategy was able to guide the quadrotor along the waypoints. Even in the presence of random external disturbance, the obtained trajectory has good quality, with no overshoots and fast time response.

It was also verified that the proposed controller took and maintained the states in a band close to $s^i_k = 0$, $i \in \{1, 2, 3\}$, for each one of the waypoints. This fact indicates the robustness of the SMC against the external disturbance $\mathbf{f}_k$.

Otherwise, it is important to note that the proposed controller doesn't consider any constraint (on position or thrust force) in the guidance algorithm, which is an important requirement of a MAV position control.

For further investigation of the proposed guidance method, an interesting future work would be its experimental test in a laboratory with controlled wind. Other interesting future work would be the study of a robust controller that also respect constraints on the thrust vector. For example, a mixed controller which combines the model predictive control (MPC) strategy with SMC.

Acknowledgment

We would like to thank “Conselho Nacional de Desenvolvimento Científico e Tecnológico (CNPq)”

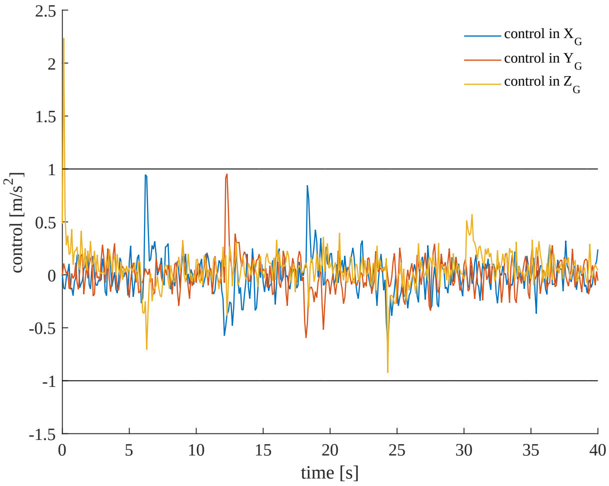

Figure 8: Control inputs in the three directions of S_{G} calculated by the sliding mode controller.

(Grant: 475251/2013).

References

Almeida, F. (2008). Waypoint navigation using constrained infinite horizon model predictive control, *AIAA Guidance, Navigation and Control Conference and Exhibit*, Honolulu, Hawaii.

Bartoszewicz, A. (1998). Discrete-Time Quasi-Sliding-Mode Control Strategies, *IEEE Transactions on Industrial Electronics* **45**(4): 633–637.

Bousson, K. and Machado, P. F. F. (2013). 4d trajectory generation and tracking for waypoint-based aerial navigation, *WSEAS Transactions on Systems and Control* **3**(8): 105–119.

Lenain, R., Thuilot, B., Cariou, C. and Martinet, P. (2006). High accuracy path tracking for vehicles in presence of sliding: Application to farm vehicle automatic guidance for agricultural tasks, *Autonomous Robots* **21**: 79–97.

Nagaty, A., Saeedi, S., Thibault, C., Seto, M. and Li, H. (2013). Control and navigation framework for quadrotor helicopters, *Journal of Intelligent and Robotic Systems* **70**(8): 1–12.

Petersen, C., Baldwin, M. and Kolmanovsky, I. (2013). Model predictive control guidance with extended command governor inner-loop flight control for hypersonic vehicles, *AIAA Guidance, Navigation, and Control (GNC) Conference*, Boston, USA.

Prado, I. A. A. and Santos, D. A. (2014). A Safe Position Tracking Strategy for Multirotor Helicopters, *22st Mediterranean Conference on Control and Automation (MED)*, Palermo, Italy.

Richards, A. and How, J. P. (2002). Aircraft trajectory planning with collision avoidance using mixed integer linear programming, *Proceedings of the American Control Conference*, Anchorage, USA.

Santos, D. A., Prado, I. A. A. and Bezerra, J. A. (2015). Waypoint-Based Guidance with Obstacle Avoidance for Multirotor Vehicles Using a Model Predictive Controller, *ABCM International Congress of Mechanical Engineering*, Rio de Janeiro, Brazil.

Santos, D. A., Saotome, O. and Cela, A. (2013). Trajectory control of multirotor helicopters with thrust vector constraints, *21st Mediterranean Conference on Control and Automation*, Platanias, Greece.